

Widespread increases in soluble phosphorus concentrations in streams across the transboundary Great Lakes Basin

Received: 7 September 2022

Nitin K. Singh¹, Kimberly J. Van Meter² & Nandita B. Basu^{1,3,4} 

Accepted: 25 July 2023

Published online: 7 September 2023

 Check for updates

Excess phosphorus from agricultural intensification has contributed to the eutrophication of rivers and lakes worldwide, including the transboundary Laurentian Great Lakes Basin. Algal blooms have surged in the past decade, threatening ecosystems, drinking water supplies and lake-dependent tourism economies in both large lakes (for example, Lake Erie) and smaller water bodies. Whereas previous research has focused mainly on phosphorus loads to Lake Erie, a comprehensive analysis of phosphorus species across the basin is lacking. Here we analyse changes in soluble reactive phosphorus and total phosphorus concentrations in over 370 watersheds across the Great Lakes Basin from 2003 to 2019. We find widespread increases in soluble phosphorus concentrations (83% of watersheds, with 46% showing significant increase), while total phosphorus concentrations are decreasing or non-significant. Utilizing random forest models, we identify small, forested watersheds at higher latitudes as the areas experiencing the largest relative increases in soluble phosphorus concentrations. Furthermore, we find winter temperatures to be a key driver of winter concentration trends. We propose that the increasing soluble phosphorus concentrations across the basin, along with warming temperatures, might be contributing to the increasing frequency and intensity of algal blooms, emphasizing the need for management strategies to prevent further water-quality degradation.

The last decade has seen an increase in the frequency and intensity of algal blooms in freshwater lakes across the world, impacting fisheries, drinking water supplies, recreational activities and contributing to economic losses of US\$4 billion annually in the United States alone^{1,2}. Algal blooms are associated with the process of eutrophication, where excess nitrogen (N) and phosphorus (P) from agricultural and urban activities are discharged to downstream waters^{3–5}. Indeed, agricultural run-off from farm fields in the United States and Canada contributes to some of the most severe and recurrent blooms in the shallow warm waters of Lake Erie, one of the five Great Lakes in the transboundary Laurentian Great Lakes Basin (GLB)^{6–8}. While bloom occurrences are

more common in agricultural and urban areas, recently blooms have also been increasing in small and large lakes across the basin^{9,10}, including two recent blooms (2012 and 2018) documented in the oligotrophic Lake Superior¹¹.

Binational targets have been developed to address water-quality challenges, including the 2012 Great Lakes Water Quality Agreement (GLWQA) that resulted in a commitment by Canada and the United States to reduce total P (TP) inputs to Lake Erie by 40% (refs. 6,12). These targets and the recurring blooms have propelled considerable research on quantifying trends in phosphorus loads from agriculturally dominated watersheds^{6,13}. Multidecadal studies in the Maumee

¹Earth and Environmental Sciences, University of Waterloo, Waterloo, Ontario, Canada. ²Department of Geography, Pennsylvania State University, University Park, PA, USA. ³Civil and Environmental Engineering, University of Waterloo, Waterloo, Ontario, Canada. ⁴Water Institute, University of Waterloo, Waterloo, Ontario, Canada.  e-mail: nandita.basu@uwaterloo.ca

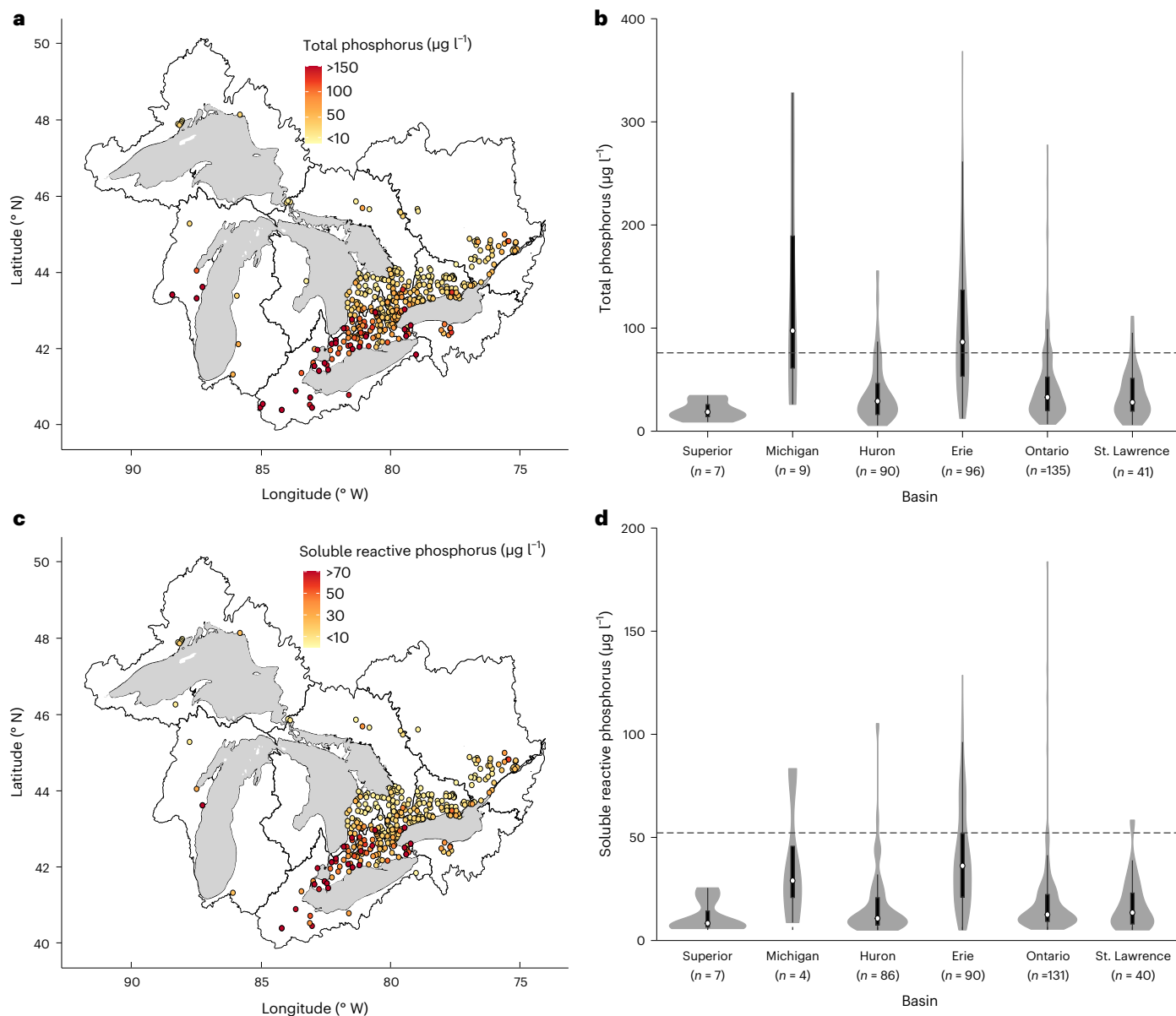


Fig. 1 | Phosphorus concentrations in streams across the Great Lakes Basin. **a,c**, Mean annual TP (**a**) and SRP (**c**) concentrations ($\mu\text{g l}^{-1}$), averaged over the last five years of data availability (2015–2019) to reflect current conditions. **b,d**, Violin plots show the distributions of observations for TP (**b**) and SRP (**d**) across the six major subbasins (Supplementary Fig. 1 for basin locations), with the number

of streams in each subbasin denoted by n . Within the violins, white-filled circles show the median value, thick lines the interquartile range and whiskers extend to a maximum of 1.5 times the interquartile range. The dashed lines indicate the eutrophic threshold of $76 \mu\text{g l}^{-1}$ for TP (**b**) and $50 \mu\text{g l}^{-1}$ for SRP (**d**).

and Sandusky watersheds in the Western Lake Erie Basin have documented a decrease in TP loads since the 1980s, in response to the 1970 GLWQA that triggered improvement of wastewater P removal technologies and ban of detergent P¹⁴. While TP has been decreasing, soluble reactive phosphorus (SRP) has been increasing since the early 2000s, and the patterns have been largely attributed to increasing tile drainage and conservation agriculture¹⁵. It has been argued that the re-eutrophication of Lake Erie following the reduction in algal blooms after the 1970s GLWQA can be attributed to these increasing trends in SRP, given greater bioavailability of soluble phosphorus^{7,8}. However, most of these studies have focused on large tributaries that drain to the lower Great Lakes, while studies across stream sizes have been missing. Exploring trends in smaller streams is critical from a management perspective, given smaller streams have been shown to exhibit higher nutrient loads relative to size and greater SRP:TP ratios¹⁶.

Of the few studies that have explored multi-watershed trends, both within the GLB and across North America, the results have been mixed. No consistent trends in TP loads were found in 18 US watersheds of western Lake Erie Basin between 1974 and 2007 (ref. 13), while decrease in loads was observed in six watersheds in the Lake Simcoe basin between 1990 to 2000 (ref. 17), and 56 watersheds in the Lake Ontario basin between 1979 and 2011 (ref. 18). Decreases in TP concentrations (1980 to 2002) were also documented in 11 forested watersheds in the oligotrophic, pre-Cambrian shield in Canada, and this was attributed to recovery from forest harvesting^{19,20}. Multi-watershed studies across the United States have documented decreasing TP and SRP concentrations in undeveloped, mixed and urban-land-use watersheds, while the absence of any significant trends was apparent in agricultural watersheds^{21,22}. In contrast, increasing TP concentrations were observed in pristine streams and lakes across the United States^{23,24}. Most

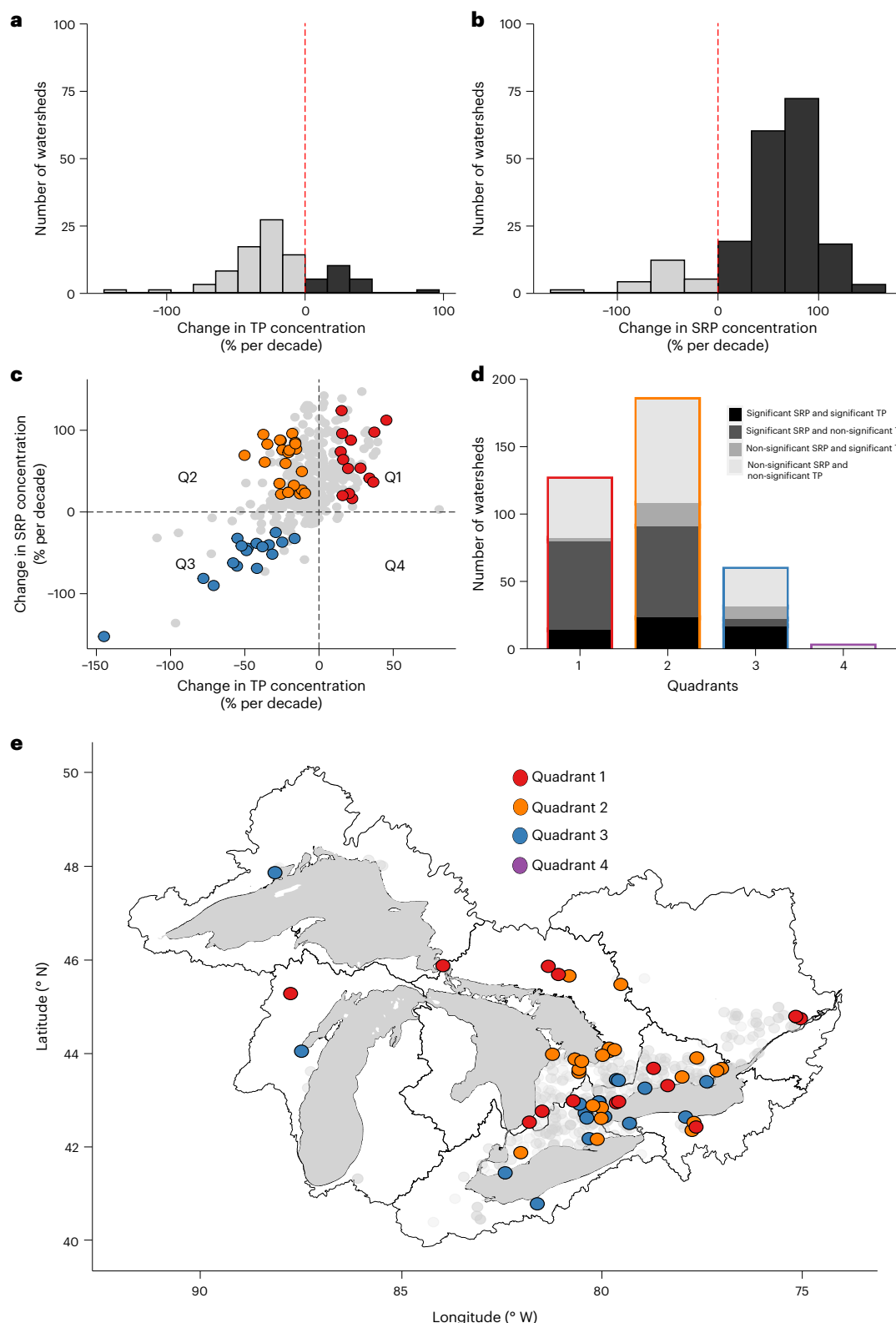


Fig. 2 | Temporal trends in soluble reactive phosphorus and total phosphorus concentrations across the Great Lakes Basin. **a,b**, Histogram of percent change in SRP (**a**) and TP (**b**) concentrations (2003–2019) for watersheds showing a significant change ($p < 0.05$). Dark and light shades of grey in **a** and **b** represent increasing and decreasing trends in concentrations, while red dashed vertical line indicates no concentration change. **c**, Quadrant plot showing the relationship between SRP and TP trends across 372 watersheds and identifying four major typologies of response: Quadrant 1 (increasing SRP and TP; Q1),

Quadrant 2 (increasing SRP and decreasing TP; Q2), Quadrant 3 (decreasing SRP and TP; Q3) and Quadrant 4 (decreasing SRP and increasing TP; Q4). Coloured filled circles represent significant ($p < 0.05$) trends and grey filled circles represent non-significant ($p > 0.05$) trends. **d**, Number of watersheds in each of the four quadrants. **e**, Spatial distribution of the typologies across the Great Lakes Basin. Coloured circles represent significant ($p < 0.05$) trends, and grey circles represent non-significant ($p > 0.05$) trends.

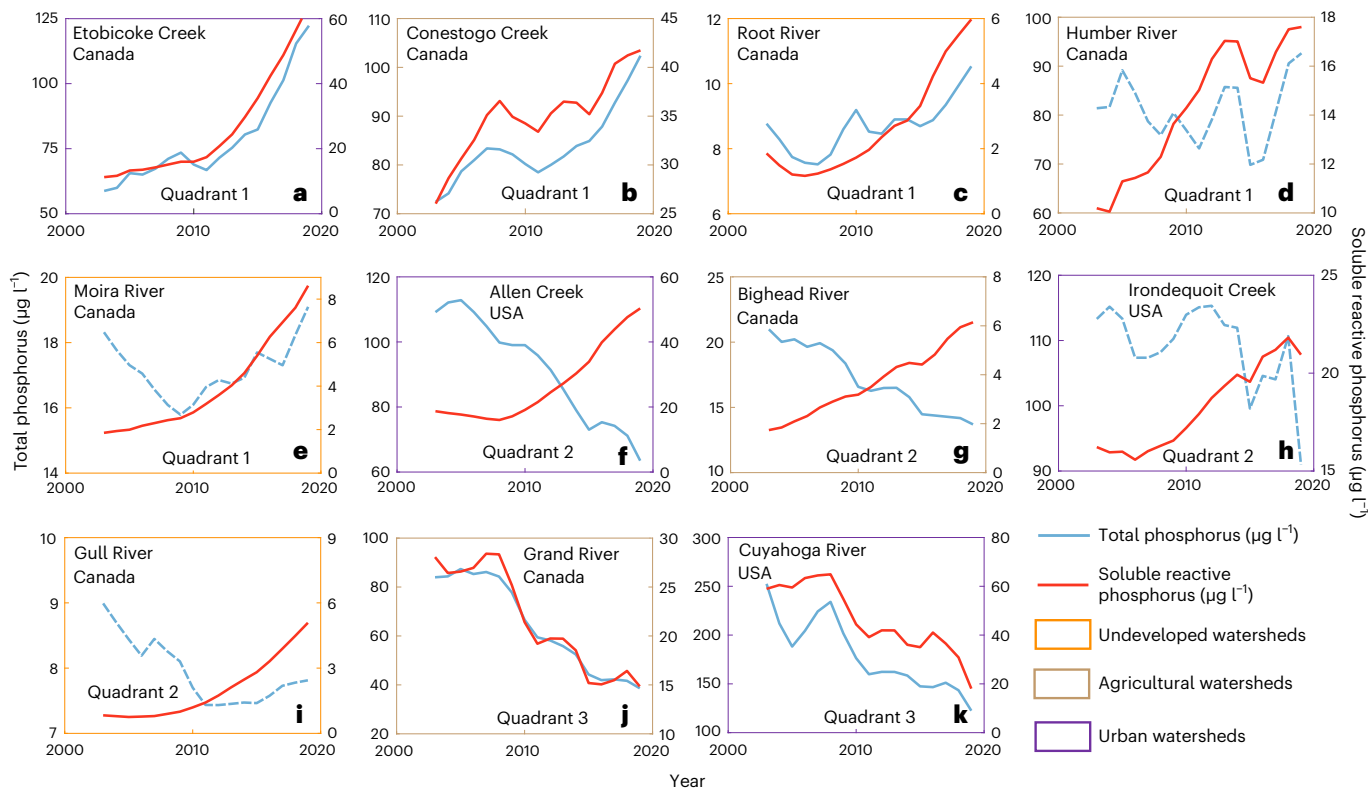


Fig. 3 | Trajectories of soluble reactive phosphorus and total phosphorus concentrations for selected watersheds. **a–c**, Quadrant 1 watersheds with significantly ($p < 0.05$) increasing SRP (red) and TP (blue) concentrations. **d,e**, Quadrant 1 watersheds with significantly ($p < 0.05$) increasing SRP and non-significant ($p > 0.05$) increase in TP concentrations. **f,g**, Quadrant 2 watersheds with significantly ($p < 0.05$) increasing SRP and decreasing TP concentrations. **h,i**, Quadrant 2 watersheds with significantly ($p < 0.05$) increasing SRP and

non-significant ($p > 0.05$) decrease in TP concentrations. **j,k**, Quadrant 3 watersheds with significantly decreasing SRP and TP concentrations ($p < 0.05$). Significant trends ($p < 0.05$) are depicted by solid lines while non-significant ($p > 0.05$) trends are depicted by dashed lines. Quadrant memberships appear to be independent of land use, as urban (indicated by a purple outline), agricultural (indicated by a brown outline) and forested/undeveloped (indicated by an orange outline) watersheds are observed in all quadrants. USA, United States of America.

of these studies have focused only on annual trends in TP, while recent basinwide analysis suggests that human activities have been altering seasonal regimes of nutrient concentrations²⁵. To date, there has been no comprehensive analysis of magnitudes and drivers of trends in SRP and TP concentrations in both US and Canadian watersheds.

Here we analyse decadal trends (2003–2019) in annual and seasonal concentrations of TP and SRP in over 370 watersheds across the transboundary GLB (~600,000 km²; Supplementary Fig. 1) to ask: (1) How do SRP and TP concentrations vary across the basin? (2) How have these concentrations changed over the last two decades? (3) What watershed characteristics (for example, climate, topography, management) are associated with these changes?

Elevated stream phosphorus concentrations across the basin

Phosphorus concentrations were found to vary widely across the GLB, with mean annual SRP and TP concentrations ranging from 2–181 $\mu\text{g l}^{-1}$ and 5–368 $\mu\text{g l}^{-1}$, respectively (Fig. 1). Seasonal concentration patterns mimic the annual patterns with a wider range of values, 2–301 $\mu\text{g l}^{-1}$ for SRP and 5–556 $\mu\text{g l}^{-1}$ for TP (Extended Data Fig. 1). The mean annual TP concentrations are greater than 76 $\mu\text{g l}^{-1}$ in 93 watersheds, while SRP concentrations are greater than 50 $\mu\text{g l}^{-1}$ in 34 watersheds, with the thresholds indicating highly productive or eutrophic systems²⁶ (Supplementary Table 1). We find that all 34 watersheds that exceed the SRP threshold also exceed the TP threshold, and 32 out of these 34 watersheds are dominated by agricultural land use. Concentrations are the highest in the Lake Erie Basin, where 57 watersheds (TP) and 22 watersheds (SRP) are over the eutrophic threshold (Fig. 1b,d;

Supplementary Table 1). While concentrations are also high in the Lake Michigan Basin, our dataset had only a limited number of monitoring points for watersheds around Lake Michigan and thus the results are not representative (Extended Data Fig. 2). Concentrations are generally lower in the Lake Ontario Basin, albeit extreme values are more common, especially for SRP in the summer months (Fig. 1d; Extended Data Fig. 1). High SRP concentrations in the summer months are probably a signal of urban wastewater discharges during times of low flows²⁵.

Decadal trends in phosphorus concentrations

We find a dominant pattern of increasing SRP (83% of the 374 watersheds with SRP data, with 46% showing significant trends; $p < 0.05$) and decreasing TP concentrations (65% of the 397 watersheds with TP data, with 18% showing significant trends; $p < 0.05$) (Fig. 2a,b and Extended Data Table 1). The patterns of increasing SRP persist at seasonal scales, with 48%, 39%, 52% and 40% of the watersheds showing significantly increasing SRP trends in winter, spring, summer and fall, respectively (Extended Data Table 1). For TP, similar to the annual scale patterns, the most dominant pattern is a lack of a significant trend across all seasons (Extended Data Table 1). The median increase in SRP concentrations across the significantly increasing watersheds is 70% per decade (Fig. 2a,b; Extended Data Table 2). Patterns are similar at the seasonal scale, with median SRP increase per decade being 68%, 81%, 75%, 80% in winter, spring, summer and fall, respectively (Extended Data Table 2).

Focusing on the 372 watersheds with available data on SRP and TP concentrations, we identified four concentration trajectory typologies (Fig. 2c–e): (1) Quadrant 1 (126 watersheds, 14 significant): SRP and TP concentrations increasing, (2) Quadrant 2 (185 watersheds,

23 significant): decreasing TP and increasing SRP, (3) Quadrant 3 (59 watersheds, 17 significant): SRP and TP decreasing and (4) Quadrant 4 (two watersheds, no significant): increasing TP and decreasing SRP (Fig. 2c–e). In Quadrant 1, we find significant ($p < 0.05$) increases in both SRP and TP concentrations (red circles in Fig. 2c) across land-use types, in urban (for example, Etobicoke Creek in the Lake Ontario Basin in Canada; Fig. 3a), agricultural (Conestogo River in the Lake Erie basin in Canada; Fig. 3b) and forested/undeveloped watersheds (Root River in Lake Huron Basin in Canada; Fig. 3c). Additionally, there are 66 watersheds in Quadrant 1 (Fig. 2d) with a significant increase in SRP ($p < 0.05$), but a non-significant ($p > 0.05$) increase in TP, which include both agricultural and forested/undeveloped basins (Humber River and the Moira River in Canada; Fig. 3d,e). Quadrant 2 contains watersheds with significant ($p < 0.05$) increases in SRP and significant ($p < 0.05$) decreases in TP concentrations (orange circles in Fig. 2c), including urban (for example, Allen Creek in the Lake Ontario basin in the United States; Fig. 3f) and agricultural watersheds (Bighead River in the Lake Huron basin in Canada, Fig. 3g). Furthermore, in Quadrant 2, there is a dominant pattern (68 watersheds; Fig. 2d) of significant SRP increase ($p < 0.05$) but non-significant TP decrease ($p > 0.05$), encompassing urban (Irondequoit Creek, United States) and forested/undeveloped (Gull River in Canada) watersheds (Fig. 3h–i). The results demonstrate increasing SRP trends across the basin regardless of land use. Only 17 watersheds in Quadrant 3 show significantly decreasing trends in SRP and TP, including the agriculture dominated Grand River watershed in Canada and the urban Cuyahoga River watershed in the United States (Fig. 3j,k).

Spatially, the typologies are distributed across the basin, with different typologies occurring in adjacent watersheds (Fig. 2e). However, a greater proportion of Quadrant 2 watersheds are found in the more northern Lake Huron, Ontario and St Lawrence basins (Extended Data Fig. 3). Additionally, Quadrant 3 watersheds have a higher median population density compared to Quadrant 1 and Quadrant 2 watersheds (Extended Data Fig. 4), indicating the influence of point source control measures such as improved wastewater treatment plant efficiency on declining trends. Conversely, Quadrant 1 and Quadrant 2 watersheds, where SRP is increasing, have a higher median forested area than Quadrant 3 watersheds.

While SRP and TP trends are variable across the basin, 67% of the 372 watersheds with data on both SRP and TP document a significant increase in the annual SRP:TP ratio across the basin (Fig. 4a,b and Extended Data Tables 1 and 2). The trend is fairly consistent across all four seasons, with median increases of 59%, 76%, 81% and 76% in winter, spring, summer and fall, respectively (Fig. 4b). A clear latitudinal gradient is apparent across the basin, with watersheds at higher latitudes showing a greater increase in the SRP:TP ratio (Fig. 4a). The latitudinal gradient and the drivers of these increases are discussed in later sections.

Watershed attributes driving phosphorus concentration trends

Our finding of decreasing or non-significant trends in TP concentrations is consistent with observations in agricultural watersheds in the western Lake Erie Basin^{14,15} and in forested and urban watersheds in Southern Ontario^{18,19}. Individual correlations revealed a lack of relationships between concentration trends and watershed drivers (Extended Data Table 3). A random forest model highlighted watershed area, latitude, slope, percent land under conservation tillage, population density and percent forested area as the top six variables that described the variability in TP trends ($R^2 = 0.34$) (Fig. 5a,c–h). The partial dependence plots further clarify that the percent decreases in TP concentrations are greatest in small (Fig. 5c), urban watersheds with high population density (Fig. 5d) and at lower latitudes (Fig. 5e). Urbanization has been shown to decrease TP concentrations in Ontario streams due to reduced fertilizer use and improvements in wastewater treatment technologies²⁷.

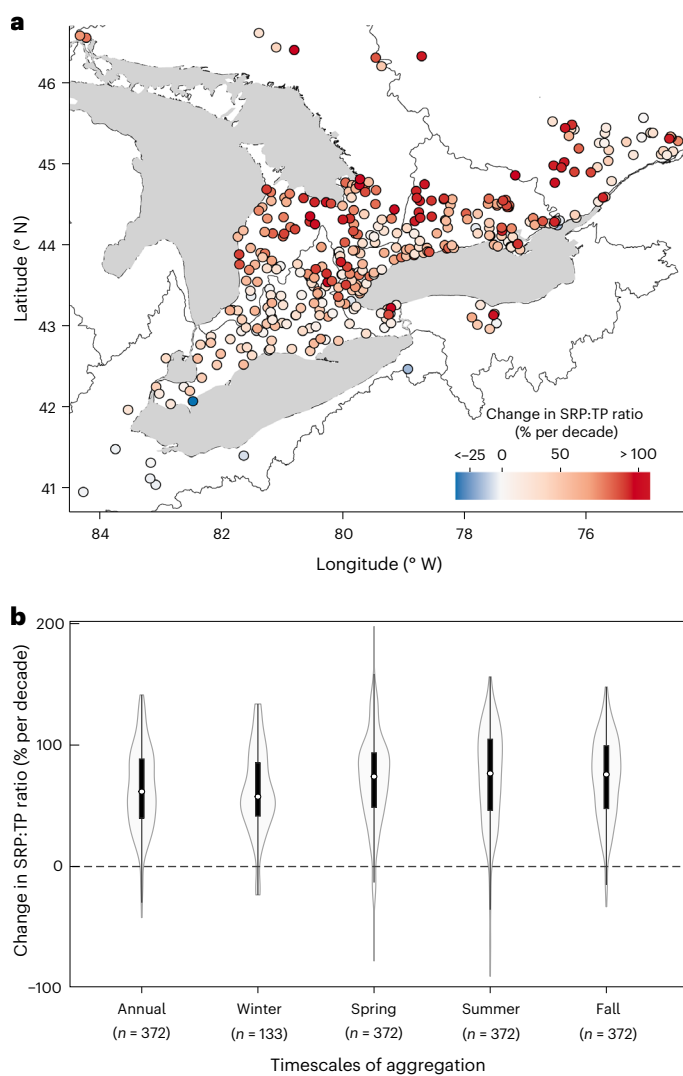


Fig. 4 | SRP:TP ratios across the Great Lakes Basin. **a**, Percent change in annual SRP:TP ratios for 372 watersheds showing greater increases in the northern watersheds. **b**, Percent change in annual and seasonal SRP:TP ratios for all watersheds documenting a significant ($p < 0.05$) increase. Violin plots show the distributions of observations for SRP:TP ratios across the basin, with the number of streams within each season and annually denoted by n . Within the violins, white-filled circles show the median value, thick lines the interquartile range and whiskers extend to a maximum of 1.5 times the interquartile range.

For SRP, our random forest model ($R^2 = 0.51$) highlighted population density, latitude, slope, watershed area, conservation tillage, slope and the agricultural area as the key drivers (Fig. 5b,i–n) of trends. The smallest SRP increases were observed in areas with the greatest population density (Fig. 5i), while the greatest increases were observed at higher latitudes (Fig. 5j) and in watersheds with steeper slopes and under conservation tillage (Fig. 5l,m). Smaller increases in SRP concentrations in urban areas can be attributed to improvements in wastewater treatment practices²⁵. Larger increases in watersheds with higher proportion of conservation agriculture practices such as no-till agriculture is consistent with previous studies that have attributed excess soluble P losses under no till to (1) maintaining macropores and thus encouraging infiltration to tile drains^{28,29} and (2) increasing soil stratification, thus promoting increased release of soluble P through subsurface pathways^{15,30,31}.

Our most interesting finding, however, is the greater increase in concentrations at high latitude watersheds, and this can be attributed

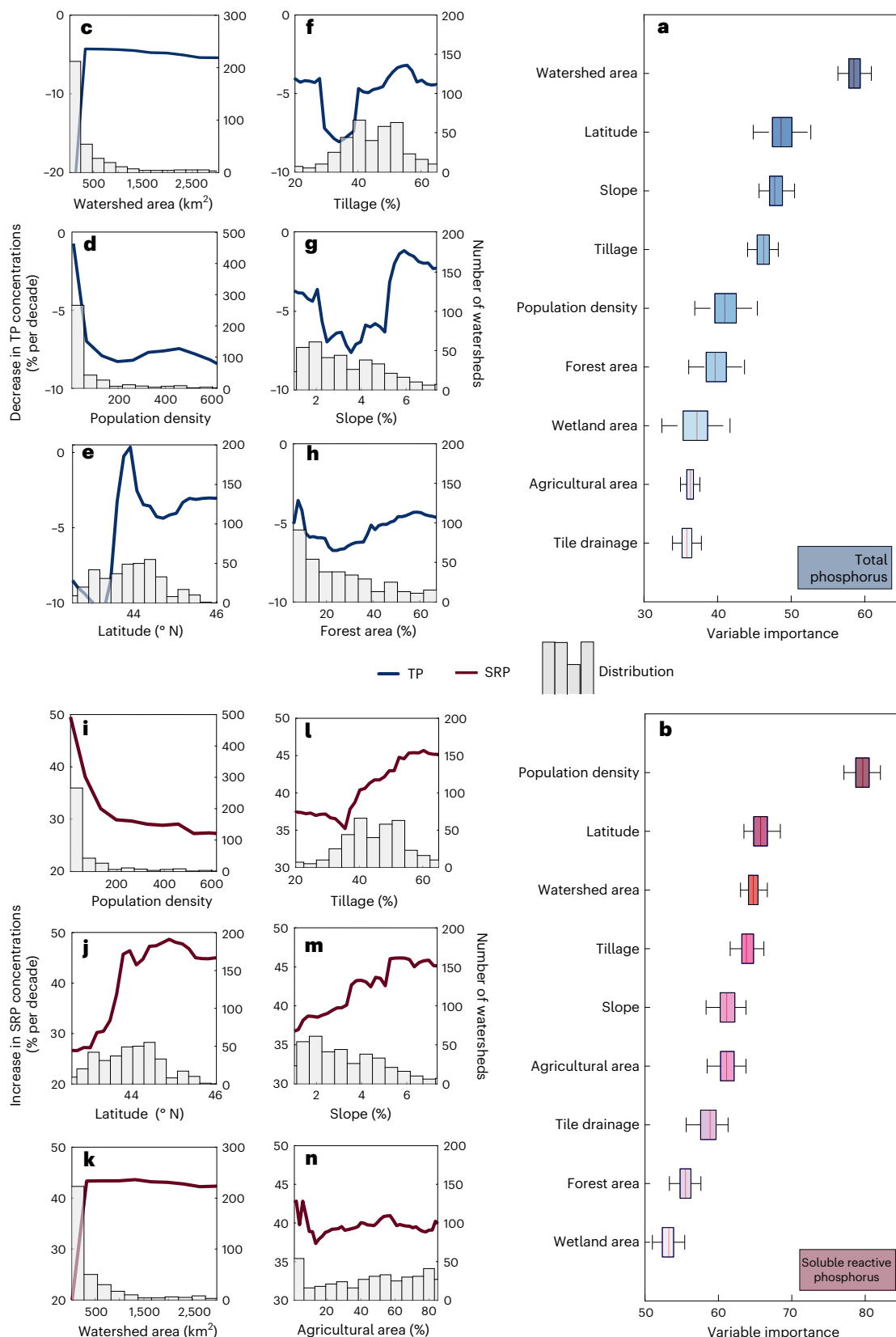


Fig. 5 | Random forest models describing trends in TP and SRP concentrations as a function of watershed attributes. **a, b,** The ranked importance of key predictors for total phosphorus (a) and soluble reactive phosphorus (b) across 100 (*n*) model runs is represented by box and whisker plots, which show the median values (vertical line in each box), the interquartile range (width of the box) and the whiskers that extend to a maximum of 1.5 times the interquartile range. Predictor boxes are shown across a colour gradient

with darker colours indicating a higher level of importance. Adjacent boxes of the same colour indicate that there is no significant ($p < 0.05$) difference in importance between those predictors (Supplementary Data). **c–n,** The partial dependence plots for change in TP (c–h) and SRP (i–n) concentrations show the marginal relationships between the predictor variables (x axis) and the percent change in concentrations (y axis). The histograms of the predictor variables are presented in grey to highlight the effect of data density on the relationships.

to both climate (for example, increased warming at higher latitudes) and land-use drivers, given the greater proportion of forested watersheds with steeper slopes at higher latitudes (Extended Data Fig. 5). Indeed, correlation analysis highlights the greatest relative increases in SRP at higher latitudes and in forested/undeveloped watersheds with high wetland coverage and steeper slopes, while the smallest increases occur in tile-drained agricultural watersheds (Extended Data Table 4). Increase in SRP concentrations in forested catchments may arise due to a reduction in acid deposition that has reduced nitrate levels in soils, thus promoting reductive dissolution of iron, which can mobilize adsorbed phosphate to be released to the streams. In a meta-analysis of 110 forested streams draining into German drinking water reservoirs, reduced acid deposition has been linked to increased mobilization of phosphate, carbon and arsenic³².

The strong latitudinal gradients in the soluble phosphorus trends alludes to large scale climate controls on the observed patterns. However, none of the climate variables emerged as important in the random forest models (Fig. 5b). To explore the effect of climate and season further, we use a combination of linear regressions and seasonal random forest models (Extended Data Fig. 6). The positive relationship between SRP increases and latitude persist with the seasonal models, with the strongest relationship emerging during winter ($p = 3.4E-8$; $r = 0.45$; Extended Data Table 4). There is a significant correlation between the temporal trends in maximum temperatures and SRP concentrations, with the strongest relationships in winter and spring (Extended Data Table 4). Temperature trends also show up as an important predictor variable in the winter random forest model (Extended Data Fig. 6). Furthermore, we find maximum winter temperatures to be increasing in nearly all watersheds and significantly ($p < 0.05$) increasing in 40% of the watersheds, while non-significant trends are apparent in the other seasons (Supplementary Table 2). Higher winter temperatures can contribute to greater frequency of freeze–thaw events contributing to an increase in the proportion of the flow routed through the subsurface^{33–35}. Given that surface flows primarily contribute to particulate P loads due to large snowmelt run-off events, while subsurface flows are driven more by thawing and contribute to dissolved P loads, it is possible that increases in winter temperatures are contributing to a preferential increase in SRP concentrations, even while TP concentrations are decreasing.

Finally, summer SRP trends show an interesting contrast with winter trends, with stronger relationships with population density and no significant relationships with temperature trends (Extended Data Fig. 6 and Extended Data Table 4). This is most likely because in these snowmelt-driven landscapes, stream concentrations are driven more strongly by non-point-source pollutants during the winter and spring months, while they are more likely impacted by point source pollution such as wastewater treatment plants during the summer months²⁵. We do find a significant relationship between summer concentration trends and increase in summer rainfall (Extended Data Table 4), albeit only 4% of the watersheds document a statistically significant increase in summer rainfall (Supplementary Table 2).

Changing climate can increase water-quality degradation

We analysed decadal trends (2003–2019) in SRP and TP concentrations across more than 350 watersheds in the Great Lakes Basin. The results revealed a widespread increase in SRP concentrations (46% of watersheds) and SRP:TP ratios (67% of watersheds). In contrast, TP concentrations have shown an increase in only 5% of watersheds and have actually decreased in 18% of them ($p < 0.05$). Notably, a clear latitudinal gradient emerged, with greater increases in SRP and SRP:TP ratios observed in the northern watersheds, characterized by steeper terrain and greater forest cover.

The observed increase in SRP concentrations can be attributed to a complex interplay of various factors related to land use, soil type and

climate: (1) implementation of agricultural practices, such as drainage and tillage, which enhance the flow through subsurface pathways, leading to the mobilization of sorbed phosphorus^{28,29,31,36,37}, (2) increased mobilization of stored phosphorus as forests recover from acidification and (3) warming winter temperatures that can activate subsurface pathways and increase the mobilization of sorbed phosphorus. Our findings indicate a significant ($p < 0.05$) increase in maximum daily winter temperatures in 40% of GLB watersheds during the study period, suggesting the potential influence of increasing freeze–thaw cycles on the increase in SRP concentrations^{33–35}.

While previous studies have reported rising SRP concentrations in certain agricultural watersheds within the Lake Erie Basin^{7,9,14,15}, our research provides evidence of a widespread increase in concentrations across diverse land uses, including agricultural, forested/undeveloped and urban watersheds. Considering the warming temperatures, increasing precipitation and rising streamflows in this region^{38,39}, a pervasive increase in SRP concentrations implies a corresponding rise in SRP loads. This, in turn, might contribute to a higher frequency and intensity of algal blooms. Indeed, we not only observed increases in concentrations but also significant increases in SRP loads in 33% of the watersheds (Extended Data Table 1).

The greater increase in SRP concentrations in forested areas can potentially contribute to the occurrence of algal blooms even in traditionally oligotrophic, pristine lakes, posing threats to drinking water sources and economies reliant on tourism. In fact, the recent surge in algal blooms in small forested lakes across the basin can be partially attributed to these increasing trends¹⁰. Furthermore, although the percentage increases may not be as pronounced in the more agricultural watersheds in the Lake Erie Basin, the already elevated SRP concentrations and SRP:TP ratios⁴⁰ in these areas mean that even a slight relative increase can have severe implications for stream and lake water quality.

Online content

Any methods, additional references, Nature Portfolio reporting summaries, source data, extended data, supplementary information, acknowledgements, peer review information; details of author contributions and competing interests; and statements of data and code availability are available at <https://doi.org/10.1038/s41561-023-01257-5>.

References

1. Ho, J. C., Michalak, A. M. & Pahlevan, N. Widespread global increase in intense lake phytoplankton blooms since the 1980s. *Nature* **574**, 667–670 (2019).
2. Hou, X. et al. Global mapping reveals increase in lacustrine algal blooms over the past decade. *Nat. Geosci.* **15**, 130–134 (2022).
3. Van Meter, K. J., Van Cappellen, P. & Basu, N. B. Legacy nitrogen may prevent achievement of water quality goals in the Gulf of Mexico. *Science* **360**, 427–430 (2018).
4. Stackpoole, S. M., Stets, E. G. & Sprague, L. A. Variable impacts of contemporary versus legacy agricultural phosphorus on US river water quality. *Proc. Natl Acad. Sci. USA* **116**, 20562–20567 (2019).
5. Basu, N. B. et al. Managing nitrogen legacies to accelerate water quality improvement. *Nat. Geosci.* **15**, 97–105 (2022).
6. Dolan, D. M. & Chapra, S. C. Great Lakes total phosphorus revisited: 1. loading analysis and update (1994–2008). *J. Great Lakes Res.* **38**, 730–740 (2012).
7. Scavia, D. et al. Assessing and addressing the re-eutrophication of Lake Erie: central basin hypoxia. *J. Great Lakes Res.* **40**, 226–246 (2014).
8. Watson, S. B. et al. The re-eutrophication of Lake Erie: harmful algal blooms and hypoxia. *Harmful Algae* **56**, 44–66 (2016).

9. Stow, C. A., Cha, Y., Johnson, L. T., Confesor, R. & Richards, R. P. Long-term and seasonal trend decomposition of maumee river nutrient inputs to western Lake Erie. *Environ. Sci. Technol.* **49**, 3392–3400 (2015).
10. Favot, E. J., Holeton, C., DeSellas, A. M. & Paterson, A. M. Cyanobacterial blooms in Ontario, Canada: continued increase in reports through the 21st century. *Lake Reservoir Manage.* <https://doi.org/10.1080/10402381.2022.2157781> (2022).
11. Sternier, R. W., Reinal, K. L., Lafrancois, B. M., Brovold, S. & Miller, T. R. A first assessment of cyanobacterial blooms in oligotrophic Lake Superior. *Limnol. Oceanogr.* **65**, 2984–2998 (2020).
12. Great Lakes Water Quality Agreement Protocol Amending the Agreement Between Canada and the United States (The Government of Canada and the Government of the United States of America, 2012); <https://www.canada.ca/en/environment-climate-change/services/great-lakes-protection/2012-water-quality-agreement.html>
13. Han, H., Allan, D. J. & Bosch, N. S. Historical pattern of phosphorus loading to Lake Erie watersheds. *J. Great Lakes Res.* **38**, 289–298 (2012).
14. Baker, D. B. et al. Phosphorus loading to Lake Erie from the Maumee, Sandusky and Cuyahoga rivers: the importance of bioavailability. *J. Great Lakes Res.* **40**, 502–517 (2014).
15. Jarvie, H. P. et al. Increased soluble phosphorus loads to lake Erie: unintended consequences of conservation practices? *J. Environ. Qual.* **46**, 123–132 (2017).
16. Mooney, R. J. et al. Outsized nutrient contributions from small tributaries to a Great Lake. *Proc. Natl Acad. Sci. USA* **117**, 28175–28182 (2020).
17. Winter, J. G. et al. Phosphorus inputs to Lake Simcoe from 1990 to 2003: declines in tributary loads and observations on lake water quality. *J. Great Lakes Res.* **33**, 381–396 (2007).
18. Stammler, K. L., Taylor, W. D. & Mohamed, M. N. Long-term decline in stream total phosphorus concentrations: a pervasive pattern in all watershed types in Ontario. *J. Great Lakes Res.* **43**, 930–937 (2017).
19. Catherine Eimers, M., Watmough, S. A., Paterson, A. M., Dillon, P. J. & Yao, H. Long-term declines in phosphorus export from forested catchments in south-central Ontario. *Can. J. Fish. Aquat. Sci.* **66**, 1682–1692 (2009).
20. O'Brien, H. D., Eimers, M. C., Watmough, S. A. & Casson, N. J. Spatial and temporal patterns in total phosphorus in south-central Ontario streams: the role of wetlands and past disturbance. *Can. J. Fish. Aquat. Sci.* **70**, 766–774 (2013).
21. Kendall, M. G. *Rank Correlation Methods*. 4th ed. (Griffin, 1970).
22. Wong, W. H. et al. Declining ambient water phosphorus concentrations in Massachusetts' rivers from 1999 to 2013: environmental protection works. *Water Res.* **139**, 108–117 (2018).
23. Stoddard, J. L. et al. Continental-scale increase in lake and stream phosphorus: are oligotrophic systems disappearing in the United States? *Environ. Sci. Technol.* **50**, 3409–3415 (2016).
24. Carleton, J. N. & Washington, B. J. Assessing evidence of phosphorus concentration trends in North American freshwaters. *J. Am. Water Resour. Assoc.* **57**, 956–971 (2021).
25. Van Meter, K. J., Chowdhury, S., Byrnes, D. K. & Basu, N. B. Biogeochemical asynchrony: ecosystem drivers of seasonal concentration regimes across the Great Lakes Basin. *Limnol. Oceanogr.* **65**, 848–862 (2020).
26. Dodds, W. K., Jones, J. R. & Welch, E. B. Suggested classification of stream trophic state: distributions of temperate stream types by chlorophyll, total nitrogen, and phosphorus. *Water Res.* **32**, 1455–1462 (1998).
27. Raney, S. M. & Eimers, M. C. Unexpected declines in stream phosphorus concentrations across southern Ontario. *Can. J. Fish. Aquat. Sci.* **71**, 337–342 (2014).
28. Boland-Brien, S. J., Basu, N. B. & Schilling, K. E. Homogenization of spatial patterns of hydrologic response in artificially drained agricultural catchments. *Hydrolog. Process.* **28**, 5010–5020 (2014).
29. Basu, N. B., Thompson, S. E. & Rao, P. S. C. Hydrologic and biogeochemical functioning of intensively managed catchments: a synthesis of top-down analyses. *Water Resour. Res.* <https://doi.org/10.1029/2011WR010800> (2011).
30. Daryanto, S., Wang, L. & Jacinthe, P. A. Meta-analysis of phosphorus loss from no-till soils. *J. Environ. Qual.* **46**, 1028–1037 (2017).
31. Macrae, M. et al. One size does not fit all: toward regional conservation practice guidance to reduce phosphorus loss risk in the Lake Erie watershed. *J. Environ. Qual.* **50**, 529–546 (2021).
32. Musolff, A., Selle, B., Büttner, O., Opitz, M. & Tittel, J. Unexpected release of phosphate and organic carbon to streams linked to declining nitrogen depositions. *Glob. Change Biol.* **23**, 1891–1901 (2017).
33. Rixon, S., Levison, J., Binns, A. & Persaud, E. Spatiotemporal variations of nitrogen and phosphorus in a clay plain hydrological system in the Great Lakes Basin. *Sci. Total Environ.* **714**, 136328 (2020).
34. Seybold, E. C. et al. Winter runoff events pose an unquantified continental-scale risk of high wintertime nutrient export. *Environ. Res. Lett.* **17**, 104044 (2022).
35. Macrae, M. L., English, M. C., Schiff, S. L. & Stone, M. Intra-annual variability in the contribution of tile drains to basin discharge and phosphorus export in a first-order agricultural catchment. *Agric. Water Manag.* **92**, 171–182 (2007).
36. Van Meter, K. J. et al. Beyond the mass balance: watershed phosphorus legacies and the evolution of the current water quality policy challenge. *Water Resour. Res.* **57**, e2020WR029316 (2021).
37. Van Staden, T. L. et al. Agricultural phosphorus surplus trajectories for Ontario, Canada (1961–2016), and erosional export risk. *Sci. Total Environ.* **818**, 151717 (2022).
38. Norton, P. A., Driscoll, D. G. & Carter, J. M. *Climate, streamflow, and lake-level trends in the Great Lakes Basin of the United States and Canada, water years 1960–2015* Scientific Investigations Report (USGS, 2019); <https://doi.org/10.3133/SIR20195003>
39. Singh, N. K. & Basu, N. B. The human factor in seasonal streamflows across natural and managed watersheds of North America. *Nat. Sustain.* **5**, 397–405 (2022).
40. Basu, N. B., Dony, J., Van Meter, K. J., Johnston, S. J. & Layton, A. T. A random forest in the Great Lakes: stream nutrient concentrations across the transboundary Great Lakes Basin. *Earth's Future* **11**, e2021EF002571 (2023).

Publisher's note Springer Nature remains neutral with regard to jurisdictional claims in published maps and institutional affiliations.

Springer Nature or its licensor (e.g. a society or other partner) holds exclusive rights to this article under a publishing agreement with the author(s) or other rightsholder(s); author self-archiving of the accepted manuscript version of this article is solely governed by the terms of such publishing agreement and applicable law.

© The Author(s), under exclusive licence to Springer Nature Limited 2023

Methods

Site selection and data sources

Phosphorus concentration data was obtained from the Provincial Water Quality Monitoring Network for Canada⁴¹ and from the US Geological Survey (USGS), Water Quality eXchange and Storage and retrieval Data Warehouse databases for the United States. Our analysis focused on Total Phosphorus (TP), which includes soluble and particulate P and orthophosphate-P (hereafter referred to as soluble phosphorus or soluble reactive phosphorus, SRP). We selected sites having observations for at least 50% of the years between 2003 and 2019 and also ensured that for every year within our time series, at least 80% of the watersheds had data (Supplementary Fig. 2). This criterion led to the selection of 397 watersheds for TP and 374 watersheds for SRP, of which 372 watersheds had both SRP and TP concentration data. Discharge data were available at only a subset of sites (SRP: 111 watersheds and TP: 121 watersheds), and this was downloaded from the Water Survey of Canada⁴² and USGS⁴³. The selected sites represented a wide range of watershed sizes (1–16,000 km², median: 195 km²), with 11 watersheds <10 km², 115 watersheds between 10 and 100 km², 189 watersheds between 100 and 1,000 km² and 84 watersheds >1,000 km². There was also a substantial variability in land use across our sites, with 239 agriculture dominated, 83 undeveloped (forest and wetland dominated), 27 urban and 50 mixed-land-use watersheds (for further details on the classification²¹, refer to Extended Data Fig. 2).

Seasonal and annual concentrations, ratios and loads

First, to understand the current status of phosphorus, we quantified the five-year mean concentrations (2015–2019) of SRP and TP for each watershed. Next, for the trend analysis, we calculated annual mean concentrations for each watershed for each year (2003–2019). We also calculated seasonal mean concentrations for each year, with seasons defined as winter (December, January, February), spring (March, April, May), summer (June, July, August) and fall (September, October, November). Data were not always present for all four seasons and years at all sites, a phenomenon that is not uncommon in monitoring datasets due to logistical limitations in data collection. To address this, we used a well-established statistical approach to fill in data gaps at a subset of sites where discharge data was available. Specifically, we used the weighted regression on time, discharge and season (WRTDS) approach to generate a daily time series of TP and SRP concentrations from sparse concentration and daily flow data⁴⁴. The WRTDS is a weighted regression model that estimates daily concentrations based on relationships developed from measured concentration, discharge, year and season. We further estimated molar ratios of SRP:TP for the days when both SRP and TP concentrations were available, and these daily ratios were used to estimate annual and seasonal mean ratios. Finally, for the subset of sites where we had access to discharge data, annual and seasonal TP and SRP loads were also estimated using the WRTDS model.

Trends in concentrations, loads and hydroclimatic variables

The time series (2003–2019) of annual and seasonal SRP (374 watersheds) and TP concentrations (397 watersheds) and SRP:TP ratios (372 watersheds) were used to test for the presence of monotonic time trends using the Mann–Kendall trend test⁴⁵. For the subset of watersheds where we had access to flow data, we also estimated temporal trends in SRP and TP loads. The Thiel–Sen’s slope was used to quantify the magnitude of the change⁴⁶, and this was divided by the mean concentration over the study duration to estimate the change as a percent. In addition, we estimated the sen slopes for trends in the hydroclimatic variables (precipitation totals, minimum and maximum temperatures), which was used in the statistical modelling of the concentration trends (Climate and landscape drivers of SRP and TP trends). The Mann–Kendall test is a widely used non-parametric method⁴⁵ to detect trends in climatic and water-quality datasets⁴⁷.

To address auto-correlation-related errors in detecting trends, we used one of the standard variance correction approaches⁴⁸. We present results with both significant ($p < 0.05$) and non-significant ($p > 0.05$) trends in our study, given issues regarding the utility of significance testing⁴⁹. We also estimated correlation between median number of observations and trends for all watersheds to confirm that trends in TP ($r = 0.006$; $p = 0.89$) and SRP ($r = -0.04$, $p = 0.35$) are not biased by the density of data.

Climate and landscape drivers of SRP and TP trends

A combination of linear regression and random forest modelling was used to explore how various landscape and climate factors impacted SRP and TP trends. The landscape variables include three geomorphic variables (latitude, watershed area, elevation and slope), three soil-related variables (percent of clay, sand, silt), latitude, population density, five land-use variables (percent of forest, wetland, agriculture, urban, open water) and three management-related variables (percent of land under tile drainage and conservation tillage). The climate variables include the sen slope of seasonal precipitation totals, sen slopes of seasonal minimum and maximum temperatures and ‘season’ as a categorical variable. Additional descriptions of the sources of the datasets for the United States and Canada are provided in Supplementary Table 3.

We first used linear regression to explore the relationships between the percent change in SRP (374 watersheds) and TP concentrations (397 watersheds) for each of the four seasons and the different landscape and climate variables. In this analysis, the landscape variables were constant across the four seasons, while the climate trends were different for each season. Correlation analysis among landscape variables was then used (Supplementary Fig. 3) to reduce the 16 variables to nine variables for random forest modelling: latitude, tile drainage, conservation tillage, watershed area, slope, population density, percent of forest, wetland, agriculture in the watershed.

We developed two sets of random forest models (RF) to understand drivers of seasonal and spatial variations in SRP (374 watersheds) and TP (397 watersheds) trends. The first set of models were developed to predict SRP and TP concentration trends for the entire dataset, as a function of climate trends, landscape variables and a categorical variable ‘season’. The second set of models (seasonal RFs) were developed one for each season, with the corresponding seasonal climate trends and the static landscape variables. RF is a non-parametric, machine learning-based multivariate regression approach that makes use of a decision tree framework to simulate dependent variables. The RF algorithm couples bootstrap aggregation with randomization and decision tree partitioning conditions. Bootstrap aggregation generates out-of-bag samples with replacement from the training dataset, simulates response for each set of samples and takes the ensemble mean of all responses⁵⁰. The RF model parameters included the number of trees generated (ntree = 2,000, default; 500) and mtry = X (number of independent variables / 3).

We used two metrics, the variable importance metric⁵⁰ and partial dependence plots⁵¹ to identify drivers of the trends. The variable importance metrics quantify how the model performance changes when the value of a variable is perturbed, such that variables that are more important are associated with a greater change in the metric. To account for model uncertainty, 100 training runs of the model were carried out, and the variable importance values for each predictor were stored across all model runs. The final rankings of predictor importance are based on the median scores across all runs. Two-factor analysis of variance (ANOVA) was used to test for significant differences between the predictor importance values of all predictor variables. The marginal influence of key predictor variables was then explored via partial dependence plots. The partial dependence plot was generated by computing the ensemble mean of simulated trends (SRP or

TP change) as a function of the corresponding climate or landscape driver, while keeping the remaining drivers unchanged, during 100 model runs.

Data availability

Phosphorus (total and orthophosphate-P) concentrations can be obtained from <https://data.ontario.ca/dataset/provincial-stream-water-quality-monitoring-network> (Canada) and <https://waterdata.usgs.gov/nwis> (United States). Flow datasets are available from https://wateroffice.ec.gc.ca/mainmenu/historical_data_index_e.html (Canada) and https://waterdata.usgs.gov/nwis/dv?referred_module=sw (United States). Monthly climate (precipitation totals, minimum and maximum air temperatures) datasets for Canada and the United States are available through <https://doi.org/10.3334/ORNLDAC/2131>. Land-use land-cover maps are available from <https://open.canada.ca/data/en/dataset/3688e7d9-7520-42bd-a3eb-8854b685fef3> (Canada) and <https://www.sciencebase.gov/catalog/item/5d4c6a1de4b01d82ce8dfd2f> (United States). Tillage datasets are available from <https://www150.statcan.gc.ca/n1/en/type/data?MM=1> (Canada) and <https://www.ctic.org/CRM> (United States). Tile-drainage maps are available from <https://geohub.lio.gov.on.ca/datasets/liotile-drainage-area/about> (Canada) and <https://figshare.com/articles/dataset/AgTile-US/11825742> (United States). Soils texture datasets are available from <https://www.fao.org/soils-portal/data-hub/soil-maps-and-databases/harmonized-world-soil-database-v12/en/> (Canada) and https://water.usgs.gov/GIS/metadata/usgswrd/XML/ds866_ssrgo_variables.xml#stdorder (United States). Population data can be downloaded from <https://www12.statcan.gc.ca/census-recensement/2011/dp-pd/index-eng.cfm> (Canada) and <https://www.census.gov/programs-surveys/decennial-census/decade.2010.html> (United States). Great Lakes Basin map can be obtained from <https://www.glc.org/greatlakesgis>.

References

41. Ontario Ministry of Environment. Provincial (stream) water quality monitoring network. <https://data.ontario.ca/dataset/provincial-stream-water-quality-monitoring-network> (Government of Ontario, 2020).
42. Historical hydrometric data website. Environment and Climate Change Canada https://wateroffice.ec.gc.ca/mainmenu/historical_data_index_e.html (2020).
43. Water data for the nation. USGS <https://waterdata.usgs.gov/nwis>? (2020).
44. Hirsch, R. M. & De Cicco, L. *User Guide to Exploration and Graphics for RivEr Trends (EGRET) and dataRetrieval: R Packages for Hydrologic Data Techniques and Methods 4-A10* (USGS, 2015); <https://doi.org/10.3133/tm4A10>
45. Kendall, M. G. *Rank correlation methods* (Griffin, 1975).

46. Sen, P. K. Estimates of the regression coefficient based on Kendall's Tau. *J. Am. Stat. Assoc.* **63**, 1379–1389 (1968).
47. Bhattacharya, R. et al. Nonlinear multidecadal trends in organic matter dynamics in Midwest reservoirs are a function of variable hydroclimate. *Limnol. Oceanogr.* **67**, 2531–2546 (2022).
48. Hamed, K. H. & Ramachandra Rao, A. A modified Mann-Kendall trend test for autocorrelated data. *J. Hydrol.* **204**, 182–196 (1998).
49. Amrhein, V., Greenland, S. & McShane, B. Scientists rise up against statistical significance. *Nature* **567**, 305–307 (2019).
50. Biau, G. & Scornet, E. A random forest guided tour. *Test* **25**, 197–227 (2016).
51. Friedman, J. H. Greedy function approximation: a gradient boosting machine. *Ann. Stat.* **29**, 1189–1232 (2001).

Acknowledgements

The research published in this paper was supported by the 'Lake Futures' project under the Global Water Futures programme, funded by the Canada First Research Excellence Fund. We thank B. Tolson and M. Han at University of Waterloo for access to and advice regarding data published in <https://lake-river-routing-products.uwaterloo.hub.arcgis.com/>.

Author contributions

N.K.S., N.B.B. and K.J.V.M. conceptualized the project. N.K.S. conducted the analyses. N.K.S. and N.B.B. analysed the figures and results. N.K.S., N.B.B. and K.J.V.M. wrote the manuscript. N.B.B. supervised and acquired funding.

Competing interests

The authors declare no competing interests.

Additional information

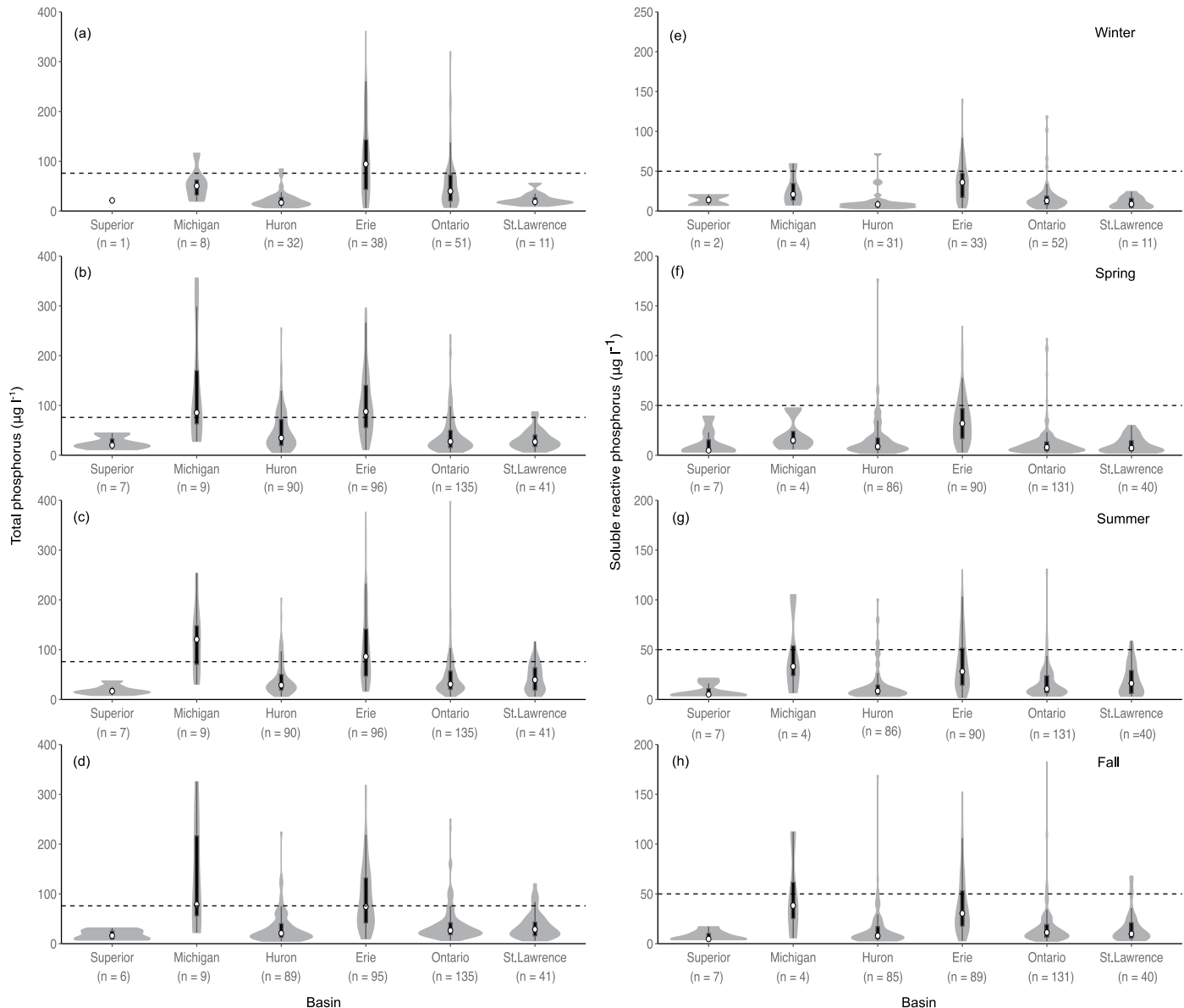
Extended data is available for this paper at <https://doi.org/10.1038/s41561-023-01257-5>.

Supplementary information The online version contains supplementary material available at <https://doi.org/10.1038/s41561-023-01257-5>.

Correspondence and requests for materials should be addressed to Nandita B. Basu.

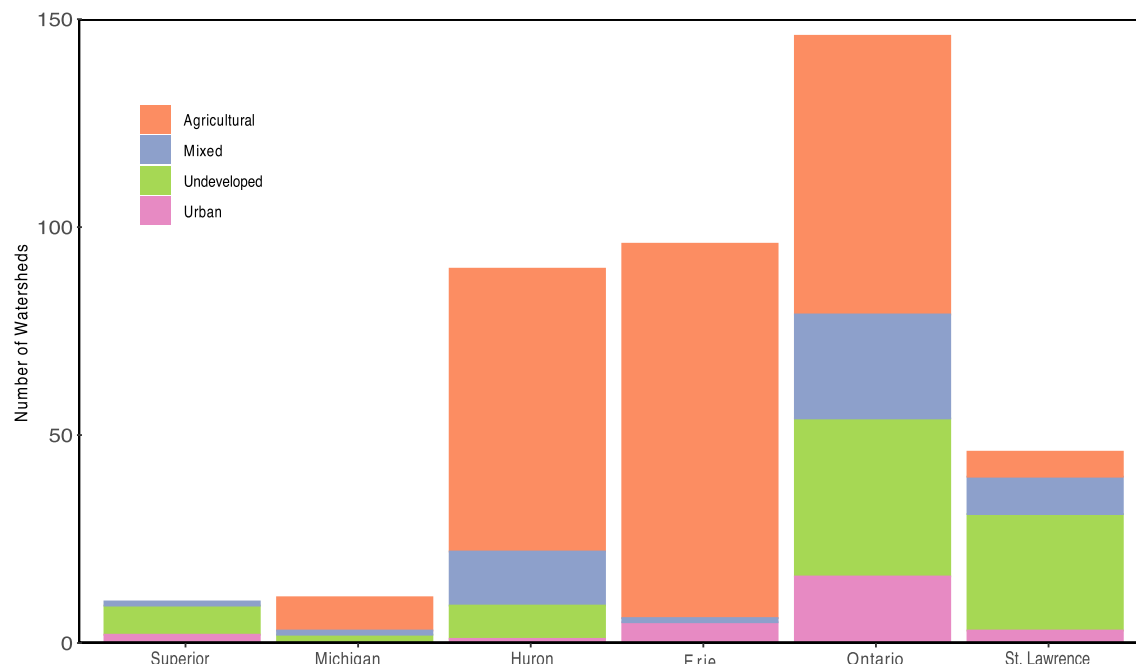
Peer review information *Nature Geoscience* thanks Robert Mooney and the other, anonymous, reviewer(s) for their contribution to the peer review of this work. Primary Handling Editor: Xujia Jiang, in collaboration with the *Nature Geoscience* team.

Reprints and permissions information is available at www.nature.com/reprints.



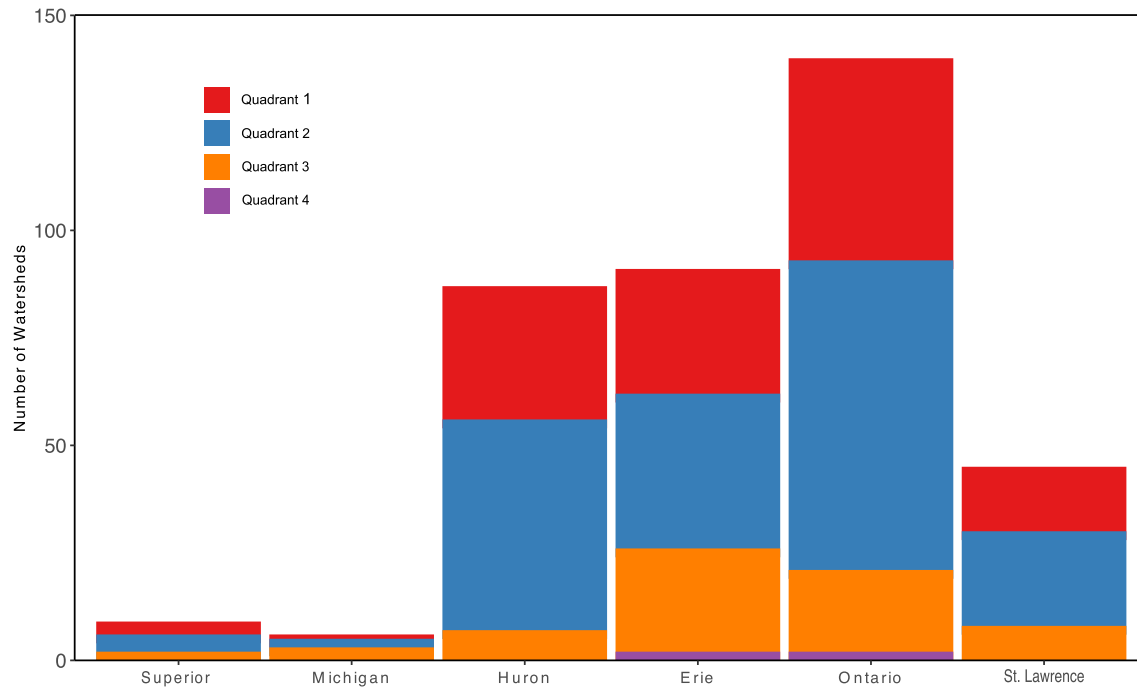
Extended Data Fig. 1 | Seasonal total phosphorus (a-d) and soluble reactive phosphorus (e-h) concentrations over the last five years across the Great Lakes Basin. Winter (a, e), Spring (b, f), Summer (c, g), Fall (d, h). Violin plots show the distributions of seasonal concentrations for (a-d) TP and (e-h) SRP across the six major subbasins (see Supplementary Fig. 1 for basin locations).

Number of streams in each subbasin is denoted by n. Within the violins, white-filled circles show the median value, thick lines the interquartile range, and whiskers extend to a maximum of 1.5 times the interquartile range. The dashed lines indicate the eutrophic threshold of $76 \mu\text{g l}^{-1}$ for TP (a-d) and $50 \mu\text{g l}^{-1}$ for SRP (e-h).

**Extended Data Fig. 2 | The distribution of land use across the Great Lakes**

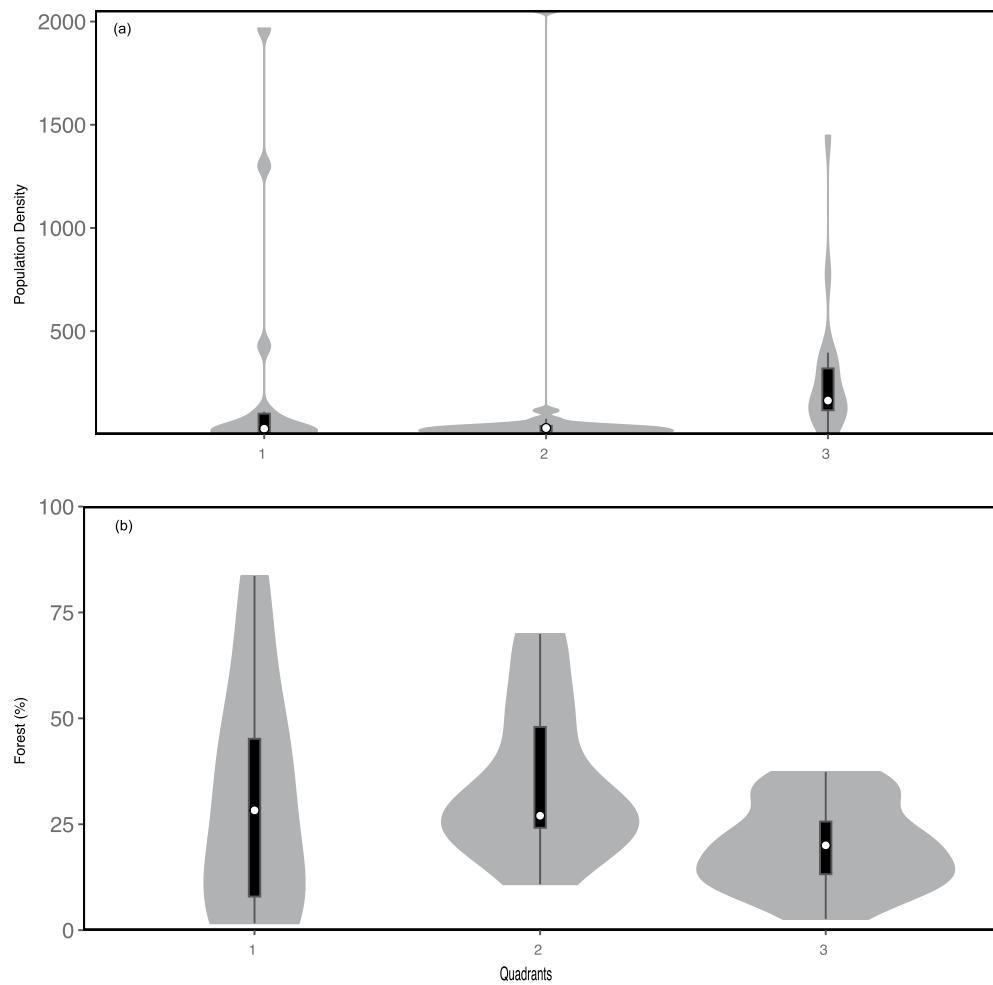
Basin. We categorized the land use and land cover maps (Canada and the United States; Supplementary Table 3) into four classes²¹: Urban [Urban >12.5% & Crop <25% & (Crop + Pasture) < 30% & Undeveloped <70%], Forested/Undeveloped

[(Forest+BarrenLand+Shrubland+Wetland+OpenWater+Grassland)>70%], Agricultural (Crop>12.5%) & (Crop + Pasture>40%) & (Undeveloped <70%), and Mixed [watersheds that do not fall into first three classes]. Mixed [watersheds that do not fall into first three classes].



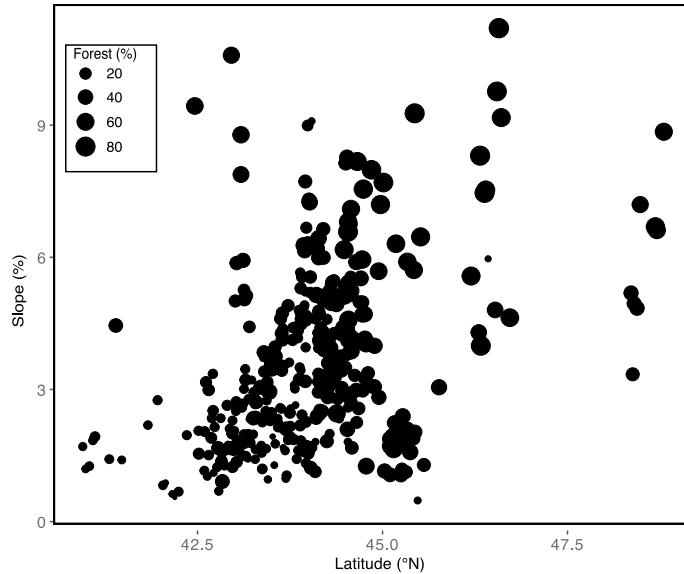
Extended Data Fig. 3 | The distribution of watershed typologies across the Great Lakes Basin. Quadrant 1 indicates watersheds where both SRP and TP are increasing, Quadrant 2 indicates watersheds where SRP is increasing and TP is decreasing, Quadrant 3 indicates watersheds where both SRP and TP are

decreasing, and Quadrant 4 indicates watersheds where SRP is decreasing and TP is increasing. Typologies are for all watersheds with significant ($p < 0.05$) or non-significant ($p > 0.05$) trends in concentrations.

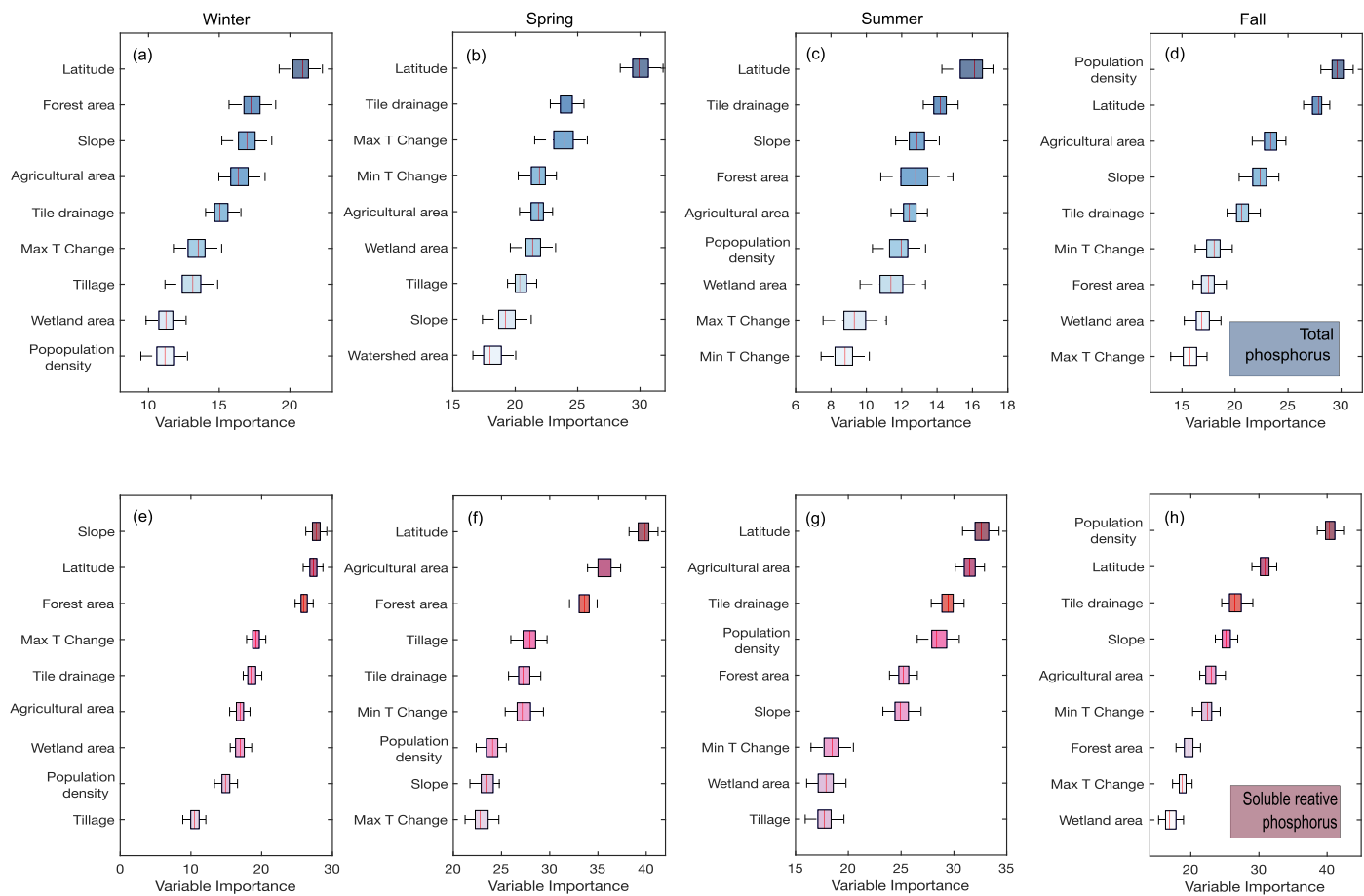


Extended Data Fig. 4 | The distribution of (a) population density and (b) forest coverage across the three typologies of trends. Note that we focused only on watersheds with significant trends, and thus Quadrant 4 is not presented. Violin plots show the distributions of observations with significant trends

($p < 0.05$), white-filled circles show the medians, thick lines the interquartile range, and whiskers extend to a maximum of 1.5 times the interquartile range. Sample sizes for (a) and (b): Quadrant 1 ($n = 14$), Quadrant 2 ($n = 23$) and Quadrant 3 ($n = 17$).



Extended Data Fig. 5 | Distribution of watersheds with forest area and mean topographic slope along the latitudinal gradient. Larger size of circles indicates greater forest cover. Overall, forest cover is greater at higher latitudes in our study watersheds.



Extended Data Fig. 6 | Variable importance plots for seasonal concentrations of total phosphorus and soluble reactive phosphorus. The ranked importance of key predictors for (a–d) total phosphorus and (e–h) soluble reactive phosphorus seasonally across 100 (n) model runs is represented by box and whisker plots, which show the median values (horizontal line in each box),

the interquartile range (width of the box), and the whiskers that extend to a maximum of 1.5 times the interquartile range. Adjacent boxes of the same color indicate that there is no significant difference in importance between those predictors ($p < 0.05$) (Supplementary Data).

Extended Data Table 1 | The proportion of watersheds (%) showing increasing and decreasing trends in annual and seasonal concentrations

Timescales of aggregation	Trend Categories	SRP Concentration	TP Concentration	SRP:TP Ratio	SRP Load	TP Load
Annual	Sig Inc*	46	5	67	33	3
	Sig Dec*	6	18	2	4	5
	Non-Sig+	48 (38/10)	77 (30/47)	31 (25/6)	63 (40/23)	92 (45/47)
Winter	Sig Inc*	48	13	56	23	4
	Sig Dec*	7	22	3	3	2
	Non-Sig+	45 (28/17)	65 (25/40)	41 (20/21)	74 (44/30)	94 (35/59)
Spring	Sig Inc*	39	4	56	27	7
	Sig Dec*	4	17	3	8	8
	Non-Sig+	57 (41/16)	79 (37/42)	41 (34/7)	65 (41/24)	85 (43/42)
Summer	Sig Inc*	52	4	56	28	4
	Sig Dec*	5	13	2	2	1
	Non-Sig+	43 (30/13)	83 (39/44)	42 (34/8)	70 (51/19)	95 (53/42)
Fall	Sig Inc*	40	6	55	25	4
	Sig Dec*	4	14	1	2	2
	Non-Sig+	56 (44/12)	80 (33/47)	44 (38/6)	73 (44/29)	94 (38/56)

*Sig (Significant) and Non-Sig+ (Non-significant) values include all watersheds with significant ($p < 0.05$) and non-significant ($p > 0.05$) trends, respectively. Numbers in parentheses represent the percent of watersheds with positive and negative non-significant ($p > 0.05$) trends, respectively.

Extended Data Table 2 | Median changes (% per decade) of annual and seasonal concentrations

Timescales of aggregation	Trend Categories	SRP Concentration	TP Concentration	SRP:TP Ratio	SRP Load	TP Load
Annual	Sig Inc*	70	21	63	68	45
	Sig Dec*	-46	-27	-17	-41	-41
	Non-Sig+	17 (22/-13)	-4 (10/-10)	15 (21/-7)	9 (20/-14)	-1 (13/-18)
Winter	Sig Inc*	68	35	59	80	75
	Sig Dec*	-47	-30	-18	-48	-61
	Non-Sig+	5 (25/-15)	-6 (12/-13)	0 (27/-9)	10 (22/-16)	-7 (13/-17)
Spring	Sig Inc*	81	23	76	91	43
	Sig Dec*	-50	-34	-16	-39	-46
	Non-Sig+	19 (33/-15)	-2 (13/-13)	28 (35/-11)	11 (30/-21)	1 (24/-22)
Summer	Sig Inc*	75	28	81	70	29
	Sig Dec*	-52	-36	-31	-52	-39
	Non-Sig+	11 (19/-9)	-1 (9/-9)	18 (22/-6)	16 (26/-8)	2 (13/-11)
Fall	Sig Inc*	80	38	76	85	59
	Sig Dec*	-46	-31	-14	-60	-60
	Non-Sig+	22 (29/-12)	-4 (11/-13)	24 (30/-10)	9 (24/-20)	-6 (10/-21)

*Sig (Significant) and +Non-Sig (Non-significant) ($p > 0.05$) values include median changes for all watersheds with significant ($p < 0.05$) and non-significant ($p > 0.05$) trends, respectively. Numbers in parentheses represent median changes for watersheds with positive and negative non-significant ($p > 0.05$) trends, respectively.

Extended Data Table 3 | Correlations (spearman coefficients and p values*) between changes in seasonal and annual TP concentrations and watershed attributes

Variables	Winter	Spring	Summer	Fall	Annual
Latitude	-0.02 (9.7E-1)	-0.05 (3.2E-1)	0.03 (4.9E-1)	0.06 (2.3E-1)	0.02 (6.9E-1)
Slope	0.17 (4.1E-2)	-0.05 (3.0E-1)	0.01 (8.2E-1)	0.01 (8.5E-1)	0.01 (8.7E-1)
Population density	0.20 (1.7E-2)	-0.03 (5.2E-1)	-0.06 (2.1E-1)	-0.23 (3.7E-6)	-0.09 (8.8E-2)
Watershed area	-0.09 (2.8E-1)	-0.08 (1.3E-1)	-0.08 (1.2E-1)	-0.02 (6.5E-1)	-0.06 (2.2E-1)
Wetland area	-0.06 (4.7E-1)	-0.03 (5.6E-1)	-0.11 (2.8E-1)	0.09 (7.3E-2)	-0.05 (3.6E-1)
Agricultural area	-0.02 (8.0E-1)	0.05 (3.2E-1)	0.05 (3.2E-1)	0.03 (5.5E-1)	0.05 (3.0E-1)
Forest area	-0.06 (4.8E-1)	0 (9.9E-1)	0.04 (4.6E-1)	0.07 (1.1E-1)	0.03 (5.6E-1)
Tillage	-0.08 (2.1E-1)	0.06 (2.3E-1)	-0.05 (3.5E-1)	-0.04 (4.4E-1)	-0.04 (4.0E-1)
Tile drainage	-0.06 (3.3E-1)	0.15 (2.0E-3)	0.10 (4.8E-2)	0.06 (2.1E-1)	0.11 (2.9E-2)
Precip Change	0.09 (2.6E-1)	-0.09 (8.8E-2)	0.06 (2.6E-1)	0.07 (1.7E-1)	0.02 (7.6E-1)
Min T Change	-0.26(1.8E-3)	-0.16 (1.7E-3)	0.02 (7.2E-1)	-0.16 (1.2E-3)	-0.05 (2.9E-1)
Max T Change	-0.19 (2.5E-2)	-0.01 (8.6E-1)	0.02 (7.3E-1)	-0.02 (6.7E-1)	-0.02 (6.8E-1)

* p values are shown in the parenthesis; significant ($p < 0.05$) values are in the bold

Extended Data Table 4 | Correlations (spearman coefficients and p values*) between seasonal and annual changes in SRP concentrations and watershed attributes

Variables	Winter	Spring	Summer	Fall	Annual
Latitude	0.45 (3.4E-8)	0.34 (1.8E-11)	0.28 (3.0E-8)	0.26 (2.2E-7)	0.33 (7.1E-11)
Slope	0.45 (2.3E-8)	0.27 (1.7E-7)	0.22 (1.8E-5)	0.24 (2.8E-6)	0.29 (1.1E-8)
Population density	-0.06 (4.7E-1)	-0.15 (4.6E-3)	-0.17 (7.1E-4)	-0.23 (6.2E-6)	-0.19 (2.6E-4)
Watershed area	-0.17 (4.9E-2)	0 (9.3E-1)	-0.12 (2.2E-2)	-0.03 (5.1E-1)	-0.07 (1.5E-1)
Wetland area	0.16 (5.9E-2)	0.19 (2.5E-4)	0.02 (7.4E-1)	0.17 (7.7E-4)	0.12 (1.6E-2)
Agricultural area	-0.45 (5.3E-8)	-0.36 (8.9E-13)	-0.14 (7.7E-3)	-0.18 (3.3E-4)	-0.26 (3.3E-7)
Forest area	0.46 (1.6E-8)	0.41 (6.8E-17)	0.27 (7.4E-8)	0.30 (2.5E-9)	0.39 (7.2E-15)
Tillage	-0.04 (6.4E-1)	-0.02 (6.7E-1)	-0.12 (2.5E-2)	-0.05 (3.4E-1)	-0.09 (1.0E-1)
Tile drainage	-0.47 (7.3E-9)	-0.25 (7.3E-7)	-0.17 (8.4E-4)	-0.24 (2.8E-6)	-0.26 (4.7E-7)
Precip Change	0.18 (4.1E-2)	0.07 (1.7E-1)	0.05 (3.3E-1)	0.08 (1.1E-1)	0.08 (1.1E-1)
Min T Change	0 (9.9E-1)	-0.20 (7.1E-5)	-0.04 (4.5E-1)	-0.16 (1.7E-3)	-0.01 (8.0E-1)
Max T Change	-0.26 (2.6E-3)	-0.28 (4.7E-8)	-0.07 (2.0E-1)	-0.10 (4.5E-2)	-0.17 (1.3E-3)

* p values are shown in the parenthesis; significant ($p < 0.05$) values are in the bold